

A Flexible Plug-and-Play Module for Generating Variable-Length

Liyang He

heliyang@mail.ustc.edu.cn
State Key Laboratory of Cognitive
Intelligence, University of Science and
Technology of China
Hefei, China

Zhenya Huang

State Key Laboratory of Cognitive
Intelligence, University of Science and
Technology of China
Hefei, China
huangzhy@ustc.edu.cn

Yuren Zhang

State Key Laboratory of Cognitive
Intelligence, University of Science and
Technology of China
Hefei, China
yurenz@mail.ustc.edu.cn

Runze Wu

NetEase Fuxi AI Lab
Hangzhou, China
wurunze1@corp.netease.com

Rui Li

State Key Laboratory of Cognitive
Intelligence, University of Science and
Technology of China
Hefei, China
ruli2000@mail.ustc.edu.cn

Enhong Chen

State Key Laboratory of Cognitive
Intelligence, University of Science and
Technology of China
Hefei, China
cheneh@ustc.edu.cn

Abstract

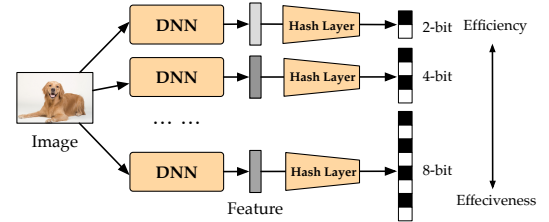
Deep supervised hashing has become a pivotal technique in large-scale image retrieval, offering significant benefits in terms of storage and search efficiency. However, existing deep supervised hashing models predominantly focus on generating fixed-length hash codes. This approach fails to address the inherent trade-off between efficiency and effectiveness when using hash codes of varying lengths. To determine the optimal hash code length for a specific task, multiple models must be trained for different lengths, leading to increased training time and computational overhead. Furthermore, the current paradigm overlooks the potential relationships between hash codes of different lengths, limiting the overall effectiveness of the models. To address these challenges, we propose the Nested Hash Layer (NHL), a plug-and-play module designed for existing deep supervised hashing models. The NHL framework introduces a novel mechanism to simultaneously generate hash codes of varying lengths in a nested manner. To tackle the optimization conflicts arising from the multiple learning objectives associated with different code lengths, we further propose an adaptive weights strategy that dynamically monitors and adjusts gradients during training. Additionally, recognizing that the structural information in longer hash codes can provide valuable guidance for shorter hash codes, we develop a long-short cascade self-distillation method within the NHL to enhance the overall quality of the generated hash codes. Extensive experiments demonstrate that NHL not only accelerates the training process but also achieves superior retrieval performance across various deep hashing models. Our code is publicly available at <https://github.com/hly1998/NHL>.

Keywords

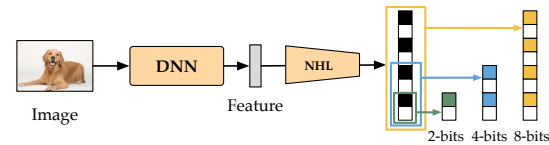
Deep Hashing, Image Retrieval, Multiple Code Learning

1 Introduction

With the accumulation of visual data on the Internet, the existing databases are becoming increasingly vast. To address the growth of data volume in large-scale image databases, hashing represents images as binary hash code for storage and search efficiency [34]. Recently, deep supervised hashing has achieved significant advancements due to its ability to extract deep features from data and utilize



(a) Deep Hashing Model with Traditional Hash Layer



(b) Deep Hashing Model with Nested Hash Layer

Figure 1: (a) The general paradigm for deep supervised hashing. We require training multiple models if we need hash codes with varying lengths for effectiveness and efficiency trade-off selection. (b) The Nested Hash Layer can concurrently generate hash codes of varying lengths in a nested fashion while only training once.

supervised signals to ensure the quality of hash codes. As shown in Figure 1 (a), the general paradigm for obtaining hash codes involves extracting data features using a deep neural network and acquiring hash codes through a hash layer¹. The hash layer usually consists of a single-layer perceptron to map the data features to a length equivalent to that of the hash codes and an operation (e.g., the sigmoid function) for acquiring the binary hash codes.

While deep supervised hashing methods have achieved notable success, they solely focus on improving the quality of hash codes with a specific code length. As shown in Figure 1 (a), each model

¹Most deep hashing methods for image retrieval adhere to this paradigm, while some works [4, 19, 39, 45] optimize the hash code in the database independently. Our work focuses on the former.

corresponds to hash codes of a specific length. This paradigm leads to two problems. On the one hand, a trade-off exists between the efficiency and effectiveness of hash codes. Within a reasonable range, shorter hash codes improve efficiency but compromise effectiveness [40]. Conversely, longer hash codes generally yield superior performance at the cost of heightened storage and computational overhead. Therefore, we must train multiple deep hashing models corresponding to different code lengths to select the most suitable code length for the current task. This will escalate training time and computational resources expenditure [46]. On the other hand, as the current deep hashing models can only generate hash codes of a single length, the potential relationships among hash codes of varying lengths are thus disregarded.

In this work, we tackle the above problems by introducing a plug-and-play module, the Nested Hash Layer (NHL), to replace the original hash layer in deep hashing models. **First**, we observe that the same backbone is employed in deep hashing to extract data features regardless of the chosen hash code length. Furthermore, longer hash codes can be viewed as supplementary descriptions of shorter ones. For example, within an 8-bit hash code, the first 4 bits can be regarded as a 4-bit hash code, while the subsequent 4 bits can be seen as complementary descriptions. Based on the two observations, the basic structure of the NHL has been proposed as shown in Figure 1 (b). This structure aims to concurrently generate hash codes of varying lengths in a nested fashion, which allows for obtaining hash codes of varying lengths from a single training session. **Second**, the basic NHL combines objectives of varying code lengths, but it cannot ensure different objectives always mutually reinforce each other. Moreover, the objectives associated with shorter hash codes become more critical as they form a part of the longer hash codes when applying NHL. This complexity underscores the need for careful consideration. To address this problem, we apply a heuristic adaptive weights strategy to the basic NHL. Specifically, we first propose the concept of domination gradient for each nested parameter in NHL. The domination gradient serves as a direction for the optimization of the corresponding parameter, prioritizing the short hash codes. Then, we monitor gradients on parameters and dynamically adjust the weights of objectives to ensure that the final optimization direction does not conflict with the domination gradient. **Third**, in contrast to the traditional hash layer, NHL can simultaneously acquire multiple lengths of hash codes. Recognizing that the relationships inherent in long hash codes can guide those of short hash codes, we propose a long-short cascade self-distillation to improve the hash codes' quality further. In summary, we make the following contributions:

- We propose a plug-and-play module called Nested Hash Layer (NHL), which can concurrently generate hash codes of varying code lengths solely by replacing the hash layer of deep supervised hashing models.
- Based on the Nested Hash Layer (NHL) architecture, we address the gradient conflicts problem by incorporating an adaptive weights strategy for learning objectives and introduce a long-short cascade self-distillation to enhance the quality of the hash codes.

- We perform comprehensive experiments about effectiveness and efficiency with various deep hashing models. The results indicate that the NHL can achieve an overall training speed increase of around 5-8 times while ensuring effective retrieval outcomes.

2 Related work

2.1 Deep Supervised Hashing

The prevailing deep supervised hashing can be roughly divided into pair-wise methods [3, 26, 30, 54–56], ranking-based methods [2, 28, 44], and proxy-based methods [9, 18, 42, 43, 50]. The objective of pair-wise methods is to ensure similar pairs have similar hash codes while dissimilar pairs have dissimilar hash codes. Ranking-based methods adopt ranking-based similarity-preserving loss terms. For instance, triplet loss [28, 44] and list-wise loss [2] are commonly used to maintain data ordering. Proxy-based methods, also known as center-based methods, have emerged as a widely acclaimed approach recently. These methods first generate each category's proxies (or hash centers). Then, they force hash codes outputted from the network to approach corresponding proxies/centers. For example, CSQ [50] generates hash centers using the Hadamard matrix or Bernoulli sampling. Based on this foundation, SHCIR [42] and MDSH [43] further incorporate semantic information of classes and impose minimum distance constraints on the hash centers, respectively.

Current deep supervised hashing methods have achieved significant success, but they only consider a model with a specific code length. This limitation leads to slow training in practical applications due to the effectiveness and efficiency trade-off with code lengths. Some works aim to create new codes through code expansion [36, 46, 47] or compression [52]. However, their focus lies in training a mapping post-model training to transform old hash codes into new hash codes. One potentially relevant approach is MAH [35]. However, it is limited to learning hash codes of only three different lengths and focuses on enhancing the accuracy of short hash codes. In contrast, our approach directly generates hash codes of arbitrary lengths during training and focuses on enhancing the overall training speed, thus presenting a fundamental distinction.

2.2 Multi-task Learning

The NHL can be partially viewed as a multi-task learning framework [25], which represents a learning paradigm where multiple distinct yet correlated tasks are simultaneously trained with a shared model. The fundamental role of our proposed NHL is to share a hash model among learning objectives of varying code lengths.

A popular line in multi-task learning is architecture design methods, such as hard parameter sharing methods [1, 22] and soft parameter sharing methods [10, 31, 38]. To cater to a wide range of deep hashing models, NHL only makes simple modifications to the hash layer. The basic structure of NHL is partially inspired by RML [24], which aims to generate representations of various lengths for diverse downstream tasks. However, RML ignores the impact of gradient conflicts and the relationships between representations of different lengths.

To address gradient or task conflicts, some methods re-weight the task losses based on specific criteria such as uncertainty [20],

gradient norm [5], or difficulty [13]. Other methods leverage gradient information to modify the gradient on the parameter update procedure. For example, PCGrad [49] projects each task gradient to the normal plane of other task gradients before combining them to form the final update vector. GradDrop [6] randomly drops out task gradients based on how much they conflict. CAGrad [29] ensures convergence to a minimum of the average loss across tasks by gradient manipulation. Nevertheless, these multi-task learning methods assume the importance of different objectives is equivalent. In NHL, the weights of objectives are different because the short hash codes appear to hold greater significance. Resolving this problem remains a further exploration.

3 METHODOLOGY

3.1 Problem Definition

Given a database $X = \{x_i\}_{i=1}^N$ comprising N images and $Y = \{y_i\}_{i=1}^N$ is the corresponding label set, deep supervised hashing targets to learn a hash function $f : x_i \mapsto h_i$ that maps each data $x_i \in X$ to a binary hash code $h_i \in \{-1, 1\}^b$, where b denotes the length of hash code. This mapping aims to preserve the pairwise similarities between the images x_i and x_j in the Hamming space, characterized by the Hamming distance for hash codes h_i and h_j . In this work, we aim to generate hash codes with m code lengths $b = \{b_k\}_{k=1}^m$. Without loss of generality, we define $b_k < b_{k+1}$. Then, the image x_i is mapped to m different lengths of hash codes, denoted as $\{h_i^{(k)}\}_{k=1}^m$.

3.2 Hash Code Generation

The process of acquiring hash codes of most deep supervised hashing methods is divided into two parts. First, a deep neural network is employed to extract the feature $v = F(x) \in \mathbb{R}^l$ given the data $x_i \in X$, where l is the dimension of v . Then, a hash layer $H(\cdot)$ is utilized to derive the hash code $h = H(v)$. In most cases, the hash layer consists of a single-layer perceptron to map the data features to a length equivalent to that of the hash code, and an operation ϕ for acquiring the hash codes. The whole process to get the hash code h can be formulated as follows:

$$h = f(x) = \phi(WF(x) + c), \quad (1)$$

where $W \in \mathbb{R}^{b \times l}$ and $c \in \mathbb{R}^b$ are the parameters in the single-layer perceptron to be learned. Current deep hashing methods usually predefine a code length b_k and then train a hash model f_k accordingly. However, in practice, the selection of an appropriate code length depends on the specific task at hand, which means we need to train multiple deep hashing models $\{f_k\}_{k=1}^m$ for different code lengths and select the most suitable one. Such an approach will increase both the training time and computational resources required. To solve this problem, we introduce NHL to replace the original hash layer in deep hashing models. In the following section, we omit the bias c and the operation ϕ for conciseness.

3.3 Basic Structure of Nested Hash Layer

Although the predefined code lengths are varying, the same backbone is employed for a specific deep hashing model. Inspired by this observation, we propose the basic structure of NHL to help deep hashing models generate hash codes with varying code lengths in one training procedure.

As shown in Figure 2 (a), NHL uses a nested parameter $\{W^{(k)}\}_{k=1}^m$ to achieve this goal without adding additional parameters to the neural network. The parameter $W^{(k)} = W_{[1:b_k]}^{(m)} \in \mathbb{R}^{l \times b_k}$ is in a nested fashion, which means $W^{(k)} \subset W^{(k+1)}$. It uses the first b_k vectors of the parameter $W^{(m)} \in \mathbb{R}^{l \times b_m}$. We can obtain the hash codes with varying lengths $\{h^{(k)}\}_{k=1}^m$ through $h^{(k)} = \phi(W^{(k)}v^T)$. Then, we aim to minimize the following objective.

$$\mathcal{L} = \sum_{i=1}^N \sum_{k=1}^m \mathcal{L}_k(h_i^{(k)}, y_i; \theta_F, W^{(k)}) \quad (2)$$

where θ_F is the parameter of backbone, and \mathcal{L}_k is the objective of a specific deep hashing model for code length b_k . In most deep hashing models, \mathcal{L}_k can be a combination of multiple objectives, such as the central similarity loss and quantization loss. As it simply involves adding the original objective of the deep hashing model, it does not alter the original optimization method. By minimizing Eq.(2), we force hash codes with varying lengths to ensure their performance.

3.4 Adaptive Weights Strategy

Although basic NHL can generate hash codes with varying lengths, we are unable to predict whether the gradients for different objectives $\{\mathcal{L}_k\}_{k=1}^m$ are mutually beneficial or detrimental. For example, in the left part of Figure 2 (b), the parameter $W^{(1)}$ is updated by three gradients $g_1^{(1)} = \frac{\partial \mathcal{L}_1}{\partial W^{(1)}}$, $g_2^{(1)} = \frac{\partial \mathcal{L}_2}{\partial W^{(1)}}$, and $g_3^{(1)} = \frac{\partial \mathcal{L}_3}{\partial W^{(1)}}$. Due to the impact of $g_2^{(1)}$, $g_3^{(1)}$, optimizing the parameters tends to proceed in a direction unfavourable to $g_1^{(1)}$ because the negative inner product between $g_1^{(1)}$ and $g_2^{(1)}$, $g_3^{(1)}$. However, The quality of the hash code $h^{(1)}$ is determined by objective \mathcal{L}_1 , which updates $W^{(1)}$ using the gradient $g_1^{(1)}$ based on the target's outcomes. Therefore, if the final optimization direction of $W^{(1)}$ diverges from $g_1^{(1)}$, it is highly probable that such a deviation will lead to a deterioration in the quality of $h^{(1)}$ because the wrong optimization direction for it.

Some multi-task learning works [6, 12, 29, 49] propose modifying the gradient on the parameter update procedure to prevent gradient conflicts. However, there exists a difference between these multi-task learning settings and NHL. Multi-task learning treats diverse learning objectives as equally important, aiming to balance various learning objectives. In NHL, the objectives corresponding to shorter hash codes appear to hold greater significance, as shorter hash codes are shared by a larger number of longer hash codes. To address this problem, we propose a heuristic adaptive weights strategy that adjusts the weight of each objective \mathcal{L}_k by monitoring the gradients. Intuitively, shorter hash codes should be granted higher optimization priority. Based on this motivation, we introduce the following definitions.

DEFINITION 1 (DOMINANT GRADIENT). Assume the gradient of \mathcal{L}_i for $W^{(k)}$ is denoted as $g_i^k = \frac{\partial \mathcal{L}_i}{\partial W^{(k)}}$. We define $g_k^{(k)} = \frac{\partial \mathcal{L}_k}{\partial W^{(k)}}$ is the dominant gradient, and $k = 1, 2, \dots, m$. For example, $g_1^{(1)}$ is the dominant gradient in Figure 2 (b).

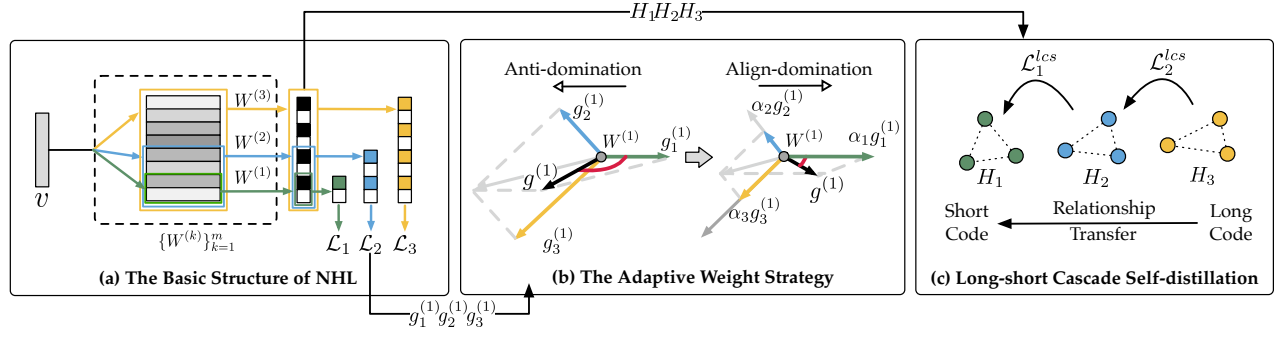


Figure 2: (a): The basic Nested Hash Layer (NHL) can generate m (here, $m = 3$) hash codes with varying lengths in one training procedure. (b) The illustration of adaptive weight strategy. Taking the $W^{(1)}$ as an example. (c) The Long-short Cascade Self-distillation transfer relationship from long hash codes to short hash codes.

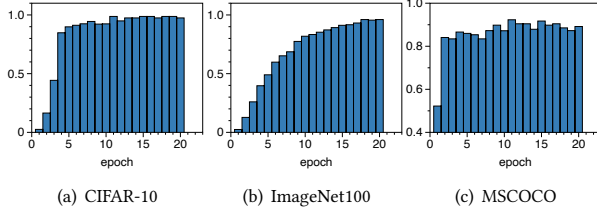


Figure 3: The probability of anti-domination occurring on the parameter $W^{(1)}$ at each epoch. We set the code lengths $m = 5$ and use CSQ as the deep hashing models on three datasets. This trend signifies a growing prevalence of anti-domination scenarios as the training progresses.

DEFINITION 2 (ANTI-DOMINATION & ALIGN-DOMINATION). Assume the gradient of \mathcal{L} for $W^{(k)}$ is $g^k = \frac{\partial \mathcal{L}}{\partial W^{(k)}}$. We define anti-domination for the update of $W^{(k)}$ if the inner product is negative between $g^{(k)}$ and the dominant gradient $g_k^{(k)}$, whereas a positive inner product is termed align-domination.

The dominant gradient $g_k^{(k)}$ serves as a guiding principle for the optimization of the parameter $W^{(k)}$. Anti-domination and align-domination are thus employed to ascertain whether the update result of $W^{(k)}$ is congruent with or divergent from the dominant gradient $g_k^{(k)}$. For example, the left part of Figure 2 (b) shows that the update of $W^{(1)}$ is anti-domination because the negative inner product between the gradient $g^{(1)}$ and $g_1^{(1)}$. We conducted an analysis to observe the occurrence of anti-domination as training progressed. Figure 3 depicts the likelihood of anti-domination occurring about parameter $W^{(1)}$ at each epoch. These results reveal the probability of anti-domination steadily rises over time, eventually stabilizing at a level exceeding 90%. This trend signifies a growing prevalence of anti-domination scenarios as the training progresses.

Our goal is to avert anti-domination for each $W^{(k)}$, for which we propose an adaptive weights strategy to ensure its realization. Specifically, as shown in the right part of Figure 2 (b), the basic

idea is to decrease the magnitudes of gradient $g_2^{(1)}$ and $g_3^{(1)}$, while increasing the magnitudes of gradient $g_1^{(1)}$. Then, $g_1^{(1)}$ can dominate the optimization direction. To achieve this goal, we tend to dynamically adjust the weight α_k for each objective \mathcal{L}_k , then the objective Eq. (2) becomes follows:

$$\mathcal{L} = \sum_{i=1}^N \sum_{k=1}^m \alpha_k \mathcal{L}_k(h_i^{(k)}, y_i; \theta_F, W^{(k)}) \quad (3)$$

To determine the value of α_k , we first present our objective in a formal manner. Similar to [5], we don't consider the full network weights and focus on the parameter in NHL, i.e., the $\{W^{(k)}\}_{k=1}^m$. Assume $\theta_{ij}^{(k)}$ is the angle between two gradients $g_i^{(k)}$ and $g_j^{(k)}$. For any k , we must ensure the following linear programming:

$$\alpha_k \|g_k^{(k)}\| + \sum_{i>k} \alpha_i \cos \theta_{ik}^{(k)} \|g_i^{(k)}\| \geq 0; k \leq m, \quad (4)$$

where notation $\|\cdot\|$ denote Frobenius norm to get the magnitude of gradients. Ensuring the validity of the inequality Eq.(4) equates to guaranteeing that the update of $W^{(k)}$ is align-domination. However, this linear programming is challenging to optimize and will incur additional time expenditure. Hence, we propose the following target:

$$\alpha_i \cos \theta_{ik}^{(k)} \|g_i^{(k)}\| + \frac{\alpha_k}{m-k} \|g_k^{(k)}\| \geq 0; k \leq i \leq m. \quad (5)$$

It is easy to demonstrate that if Eq. (5) holds for any k and i , then Eq. (4) also holds. Through Eq.(5), we can get the range of α_i . Without loss of generality, we first set $\alpha_1 = 1$ for the shortest code' objective \mathcal{L}_1 , as normalization can subsequently be applied. Then we introduce $\alpha_i^{(k)}$ denote only consider to ensure that L_i and L_k satisfy Eq. (5) on $W^{(k)}$. Using $\cos \theta_{ik}^{(k)} = \frac{g_i^{(k)} \cdot g_k^{(k)}}{\|g_i^{(k)}\| \|g_k^{(k)}\|}$ and re-arranging terms, we then get:

$$\alpha_i^{(k)} (-g_i^{(k)} \cdot g_k^{(k)}) \leq \frac{\alpha_k}{m-k} \|g_k^{(k)}\|^2; k \leq i \leq m. \quad (6)$$

If $g_i^{(k)} \cdot g_k^{(k)} \geq 0$, because $\alpha_j > 0$ for $j = 1, 2, \dots, m$, the inequality invariably holds. Then we set $\alpha_i^{(k)} = 1$. If the case that $g_i^{(k)} \cdot g_k^{(k)} < 0$,

we can get:

$$\alpha_i^{(k)} \leq \frac{\alpha_k}{k-m} \frac{\|g_k^{(k)}\|^2}{g_i^{(k)} g_k^{(k)}}; k \leq i \leq m. \quad (7)$$

Since our target is to minimize the impact on other optimization objectives while avoiding anti-domination as much as possible, we equate the terms on both sides of Eq.7, ultimately deriving the solution:

$$\alpha_i^{(k)} = \begin{cases} 1 & \text{if } g_i^{(k)} \cdot g_k^{(k)} \geq 0 \\ \frac{\alpha_k}{k-m} \frac{\|g_k^{(k)}\|^2}{g_i^{(k)} g_k^{(k)}} & \text{if } g_i^{(k)} \cdot g_k^{(k)} < 0; k \leq i \leq m \end{cases} \quad (8)$$

Then, consider \mathcal{L}_i and all $\mathcal{L}_k, k < i$, the α_i is as follows:

$$\alpha_i = \min(\alpha_i^{(1)}, \alpha_i^{(2)}, \dots, \alpha_i^{(i)}). \quad (9)$$

In each training step, we dynamically compute the $\{\alpha_k\}_{k=1}^m$ using Eq. (8) and Eq. (9). The computation complex is $O(lb_m m^2)$, where l is the dimension of data feature v and b_m is the longest code length. We conducted an experiment in Section 5.5 to demonstrate that incorporating the adaptive weights strategy increases the training time per step by approximately 11.15%.

3.5 Long-short Cascade Self-distillation

Compared to the traditional hash layer, the deep hashing model with NHL can simultaneously generate hash codes with varying code lengths. This prompts us to consider the intrinsic connections among hash codes of varying lengths. We find a teacher-student relationship is established between long hash codes and short hash codes. Therefore, As shown in Figure 2 (c), we propose the long-short cascade self-distillation method, leveraging long hash codes to enhance the performance of short hash codes in a cascade manner.

Specifically, for arbitrary image x_i , through the NHL we can get its corresponding hash codes $\{h_i^{(k)}\}_{k=1}^m$. Let $H_k = [h_1^{(k)}, h_2^{(k)}, \dots, h_B^{(k)}] \in \{-1, 1\}^{B \times b_k}$ denote the matrix of hash codes with length b_k in current training batch, and B is the batch size. Then the self-distillation objectives can be formulated as:

$$\mathcal{L}_k^{lcs} = \frac{1}{B} \left\| \frac{h_i^{(k)} H_k^T}{\|h_i^{(k)} H_k^T\|} - \frac{h_i^{(k+1)} H_{(k+1)}^T}{\|h_i^{(k+1)} H_{(k+1)}^T\|} \right\|^2. \quad (10)$$

Eq.(10) can be viewed as transferring the relationship between $h_i^{(k+1)}$ and other hash codes of length b_{k+1} to the relationship between $h_i^{(k)}$ and other hash codes of length b_k . Besides, we stop the gradient propagation of the long hash codes $h_i^{(k+1)}$ and $H_{(k+1)}$ to ensure that the learning of relationships is unidirectional. In other words, we only allow the shorter hash codes to learn from the relationships of the longer hash codes. By introducing the long-short cascade self-distillation into the optimization procedure, the objective Eq.(3) becomes:

$$\mathcal{L} = \sum_{i=1}^N \sum_{k=1}^{m-1} \alpha_k (\mathcal{L}_k + \lambda \mathcal{L}_k^{lcs}) + \sum_{i=1}^N \alpha_m \mathcal{L}_m, \quad (11)$$

where λ is a hyper-parameter. This method readily allows for expansion. For instance, one could explore the relationship between h_k

Algorithm 1 The training algorithm with NHL

Input: training samples $X = \{x_1, x_2, \dots, x_N\}$, the hyper-parameters λ .

- 1: Initialization: the parameter of the deep hashing model $\{\theta_F, W\}$, $\alpha_k = 1 \forall k$.
- 2: **repeat**
- 3: draw a mini-batch $\{x_1, x_2, \dots, x_B\}$ from X to compute $\{\mathcal{L}_k\}_{k=1}^m$ using standard forward propagation algorithm
- 4: **for** each $k \in \{1, 2, \dots, m\}$ **do**
- 5: **for** each $i \in \{1, 2, \dots, m\}$ **do**
- 6: obtain $g_i^{(k)}$ by computing standard gradients $g_i^{(k)} = \frac{\partial \mathcal{L}_i}{\partial W^{(k)}}$ {Only calculating the gradients on $\{W^{(k)}\}_{k=1}^m$ }
- 7: **end for**
- 8: **end for**
- 9: compute $\{\alpha_k\}_{k=1}^m$ by Eq. (9) and Eq. (8)
- 10: renormalize $\{\alpha_k\}_{k=1}^m$ so that $\sum_{k=1}^m \alpha_k = m$
- 11: update parameters of the deep hashing model by minimizing Eq. (11) using the standard backpropagation algorithm
- 12: **if** achieved a smaller \mathcal{L}_k **then**
- 13: record the current model parameters $\theta_F^{(k)}, W^{(k)}$ for the model of length b_k .
- 14: **end if**
- 15: **until** converged

Output: parameters of deep hashing model $\{\theta_F^{(k)}\}_{k=1}^m$ and $\{W^{(k)}\}_{k=1}^m$

and h_{k+a} , where a is an integer, but this is not the central concern of our work.

We renormalize the weights α_k in each step so that $\sum_{k=1}^m \alpha_k = m$ to decouple gradient re-weight from the global learning rate. Besides, in the training procedure, note that the minimum of \mathcal{L} does not necessarily imply that each $\{\mathcal{L}_k\}_{k=1}^m$ is at its minimal value during the training process. Therefore, we propose a trick for our training procedure. Throughout the training, we monitor the value of each \mathcal{L}_k and save the model parameters when each \mathcal{L}_k reaches its minimum to output the corresponding hash codes $h^{(k)}$. We summarize the whole algorithm in Algorithm 1. We present the training algorithm of our proposed NHL in Algorithm 1. In lines 12-14 of Algorithm 1, when a smaller \mathcal{L}_k is achieved, We record the current model parameters θ_F and W as the parameters of the model with a length of b_k , denoted as $\theta_F^{(k)}$ and $W^{(k)}$.

4 Discussion & Future Direction

The proposed NHL module can be integrated into the majority of deep supervised hashing models [2, 3, 9, 16, 18, 26, 28, 30, 42–44, 50, 54–56]. A characteristic feature of these models is that both the database data and the query data rely on the same deep hashing network for hash code generation, known as symmetric method. Nevertheless, we must clarify that NHL is not applicable to some deep supervised hashing models [4, 19, 39, 45], which are known as the two-step method or asymmetric method. These models are characterized by their direct or indirect optimization of hash codes in the database rather than obtaining hash codes through the output of the deep neural network. They solely utilize deep neural

networks for processing query images and obtaining their hash codes. Exploring how to adapt NHL to these models represents a worthwhile direction for future research.

Besides, in our earlier experiments, we also explored applying NHL in deep unsupervised hashing models. However, we found that the NHL does not consistently achieve significant improvements in these models. This underscores the importance of supervised signals in multiple objective learning. Exploring how to integrate the concept of NHL into deep unsupervised hashing models remains a worthwhile pursuit.

5 Experiments

5.1 Experiment Settings

5.1.1 Dataset. We conducted experiments on three widely used datasets in deep hashing for evaluation. **CIFAR-10** [23] consists of 60,000 images from 10 classes. Following [3], we randomly select 1,000 images per class as the query set, and 500 images per class as the training set, and use all remaining images as the database. **ImageNet100** is a subset of ImageNet [7] with 100 classes. We follow the settings from [9] and randomly select 100 categories. Then, we use all the images of these categories in the training set as the database and the images in the validation set as the queries. Furthermore, we randomly select 13,000 as the training images from the database. **MSCOCO** [27] is a large-scale dataset for object detection, segmentation, and captioning. We consider a subset of 122,218 images from 80 categories, as in previous works [37]. We randomly select 5,000 images from the subset as the query set, and use the remaining images as the database. For training, we randomly select 10,000 images from the database. As in most deep hashing settings, two samples are viewed as similar if they correspond to the same label on CIFAR-10 and ImageNet100. For multi-label datasets MSCOCO, two samples are considered similar if they share at least one common label.

5.2 Evaluation Metric

We employed the mean Average Precision at the top K ($mAP@K$) as the evaluation metric. Specifically, we utilized $mAP@5000$ for MSCOCO and $mAP@1000$ for both CIFAR-10 and ImageNet100, following the settings used in previous studies [9, 37]. Unless otherwise specified, we set the hash code lengths $b \in \{8, 16, 32, 64, 128\}$ for the following experiments, as these lengths are prevalently used in previous works.

5.3 Baselines and Training Details

We considered the following deep supervised hashing models, including DSH [30], DTSH [44], LCDSH [55], DCH [3], CSQ [50], DPN [9], and MDSH [43]. In subsequent experiments, we use w/o NHL to represent deep hashing models without using NHL, and w/ NHL means deep hashing models use NHL to replace the original hash layer. We carefully implemented all models using Pytorch and conducted experiments on an NVIDIA Geforce RTX4090 GPU. We used ResNet50 [14] as the backbone to extract 2048-D image features and try our best to re-implement the previous methods. The batch size B was set to 64. When deep hashing models applied NHL, we used the Adam optimizer [21] and selected the learning rate from $\{10^{-4}, 10^{-5}\}$. The hyper-parameter λ was selected from

$\{10^1, 10^0, 10^{-1}, 10^{-2}, 10^{-3}\}$. We perform the grid search method on different cases for the best combination.

5.4 Performance on Deep Hashing Models

In this experiment, we compared the $mAP@K$ of different deep supervised hashing models on three datasets. Table 1 presents an overview of the results. We use “w/o NHL” to denote the deep hashing model without using NHL and use “w/ NHL” to denote the deep hashing model that uses NHL to replace the original hash layer. In its original paper, MDSH [43] does not present methods for processing multi-label datasets. Thus, we cannot get the results of MDSH on the MSCOCO dataset.

Table 1 shows the results. We use bold numbers to indicate statistically significant improvements when utilizing NHL compared to not using NHL, with $p < 0.05$ based on a two-tailed paired t-test. We can find the following observations: (i) Globally, the implementation of the NHL leads to an average improvement of 4.46% (4.69% in CIFAR-10, 6.03% in ImageNet100, and 2.35% in MSCOCO). Besides, there are 72% of cases that achieve a significant performance boost based on the two-tailed paired t-test. Conversely, only a few cases achieve a decline, with most drops of 1.37% occurring in the DTSH model when NHL is applied to the ImageNet100 dataset using a 128-bit code. Thus, we can demonstrate that NHL can yield significant improvements in the majority of cases. (ii) Deep hashing models with NHL improve significantly when the hash code length is short in some datasets. For example, in the case of 8-bit, employing NHL can increase 18.7% and 7.32% enhancement on ImageNet100 and MSCOCO datasets, respectively. This is attributed to the adaptive weights strategy and long-short cascade self-distillation introduced for the NHL structure, ensuring optimization for short hash codes and leveraging the relationships in long hash codes to enhance the performance of short hash codes. (iii) It is delightful to note that NHL can address the curse of dimensionality of hash code, signifying that as the code length expands to a certain dimension, the code quality commences to deteriorate in some deep hashing models. For example, without NHL, the quality of hash codes in DSH experiences a marked decline when transitioning from 64 bits to 128 bits on the CIFAR-10 dataset. In contrast, with the incorporation of the NHL, this result undergoes a substantial improvement.

5.5 Efficiency Analysis

In this experiment, we evaluated the deep hashing model’s training time and memory usage. We recorded the total training time for the hashing model of five code lengths and recorded the maximal memory usage.

Table 2 displays the results, where we selected CSQ and DCH as the deep hashing models. These results demonstrate that the employment of the NHL incurs negligible additional memory expenses. This is attributed to the fact that during the training process, the primary memory usage stems from the parameters of the neural network, while the additional memory occupied by the target loss is relatively minimal. Meanwhile, the incorporation of the NHL can significantly enhance the overall training speed. Specifically, it achieved an average training speedup of 5.94 \times , 6 \times , and 5.31 \times on the CIFAR-10, ImageNet-100, and MSCOCO datasets, respectively, across the two deep hashing models. In conjunction with the

Data	Model	w/o NHL						w/ NHL					
		8 bits	16 bits	32 bits	64 bits	128 bits	avg.	8 bits	16 bits	32 bits	64 bits	128 bits	avg.
CIFAR-10 (mAP@1000)	DSH	0.690	0.731	0.740	0.727	0.381	0.654	0.717	0.732	0.744	0.743	0.749	0.737 (+12.8%)
	DTSH	0.754	0.778	0.799	0.831	0.811	0.745	0.766	0.790	0.802	0.822	0.836	0.771 (+3.51%)
	LCDSH	0.715	0.771	0.817	0.826	0.854	0.797	0.775	0.799	0.825	0.839	0.868	0.821 (+3.08%)
	DCH	0.776	0.802	0.829	0.830	0.825	0.812	0.787	0.810	0.833	0.843	0.844	0.823 (+1.36%)
	CSQ	0.762	0.786	0.798	0.798	0.807	0.790	0.792	0.802	0.818	0.828	0.838	0.816 (+3.21%)
	DPN	0.703	0.757	0.790	0.804	0.819	0.775	0.729	0.765	0.795	0.826	0.824	0.788 (+1.71%)
	MDSH	0.755	0.808	0.829	0.844	0.832	0.814	0.762	0.811	0.838	0.852	0.861	0.825 (+1.40%)
ImageNet100 (mAP@1000)	DSH	0.703	0.808	0.827	0.828	0.822	0.797	0.755	0.816	0.829	0.838	0.841	0.817 (+2.41%)
	DTSH	0.432	0.710	0.770	0.784	0.803	0.794	0.552	0.714	0.766	0.788	0.792	0.803 (+1.11%)
	LCDSH	0.248	0.395	0.542	0.608	0.692	0.450	0.422	0.568	0.628	0.657	0.692	0.593 (+19.4%)
	DCH	0.776	0.834	0.845	0.859	0.848	0.832	0.809	0.842	0.855	0.860	0.863	0.846 (+1.65%)
	CSQ	0.456	0.822	0.860	0.877	0.878	0.778	0.495	0.825	0.873	0.880	0.882	0.787 (+1.59%)
	DPN	0.436	0.827	0.864	0.870	0.877	0.775	0.487	0.829	0.860	0.877	0.881	0.788 (+1.50%)
	MDSH	0.785	0.845	0.874	0.895	0.894	0.859	0.794	0.851	0.878	0.884	0.896	0.861 (+0.23%)
MSCOCO (mAP@5000)	DSH	0.685	0.722	0.757	0.779	0.769	0.743	0.714	0.735	0.764	0.779	0.789	0.756 (+1.77%)
	DTSH	0.706	0.770	0.810	0.823	0.831	0.788	0.751	0.793	0.819	0.826	0.823	0.803 (+1.86%)
	LCDSH	0.687	0.769	0.787	0.825	0.836	0.781	0.713	0.773	0.794	0.820	0.828	0.786 (+0.55%)
	DCH	0.695	0.756	0.762	0.777	0.734	0.745	0.723	0.769	0.786	0.788	0.789	0.771 (+3.51%)
	CSQ	0.596	0.750	0.847	0.877	0.871	0.788	0.659	0.778	0.847	0.878	0.881	0.809 (+2.58%)
	DPN	0.575	0.757	0.828	0.862	0.863	0.777	0.638	0.769	0.837	0.863	0.872	0.796 (+2.44%)

Table 1: The mAP@K comparison results on CIFAR-10, ImageNet100, and MSCOCO datasets when different deep hashing models used the original hash layer (w/o NHL) or NHL (w/ NHL). We employ bold numbers to indicate statistically significant enhancements when utilizing NHL compared to when not using NHL, with $p < 0.05$ based on a two-tailed paired t-test.

Data	Model	Time (hours)		Memory (GiB)	
		w/o NHL	w/ NHL	w/o NHL	w/ NHL
CIFAR-10	CSQ	0.455	0.083 (5.48×)	12.822	12.868
	DCH	0.543	0.085 (6.39×)	12.820	12.836
ImageNet100	CSQ	4.520	0.664 (6.81×)	12.923	13.139
	DCH	6.025	1.161 (5.19×)	12.914	12.956
MSCOCO	CSQ	1.019	0.202 (5.05×)	12.906	13.067
	DCH	5.475	0.981 (5.58×)	12.886	12.926

Table 2: The efficiency evaluation on three datasets. We record the total training time for the deep hashing model of five code lengths and the maximal memory usage.

conclusions drawn from the previous experiment, this evidences that NHL can effectively expedite the training procedure without compromising the quality of hash codes.

Besides, we further analyze the average time per epoch during training across different NHL variants. Figure 4 displays the results of CSQ and DCH. Compared to deep hashing models without NHL (w/o NHL), the use of NHL-basic and NHL w/o A resulted in an increase in training time of 3.37% and 6.87%, respectively. This indicates that introducing a basic NHL structure and employing self-distillation do not significantly extend the duration of each epoch. Furthermore, compared to models without using NHL (w/o NHL), those with NHL w/o D and w/ NHL experience an average increase in training time of 11.15% and 13.75%, respectively. This increase is primarily attributed to our adaptive strategy that explicitly monitors and analyzes parameters within NHL rather than across the entire model.

5.6 Ablation Study

To analyze the influence of each component in the NHL, we conducted an ablation study on these models to investigate their impact. We devised several variants for the NHL, namely (i) NHL-basic: directly use Eq (2) to optimize the deep hashing model, (ii) NHL w/o A: without using the adaptive weights strategy, (iii) NHL w/o D: without using the long-short cascade self-distillation. We present the results CSQ on CIFAR-10 and ImageNet100 in Figure 5. We can find that employing NHL-basic does not enhance the performance of hash codes compared to using the original hash layer. This indicates that simply jointly learning the objective function like Eq.(2) is insufficient. Furthermore, the adaptive weight strategy (NHL w/o D) and the long-short cascade self-distillation (NHL w/o A) enhance the performance of NHL-basic. These results underscore the significance of contemplating gradient optimization scenarios and facilitating short hash codes to learn from long code relationships. Finally, a notable enhancement can be achieved by simultaneously considering these two factors (w/ NHL).

5.7 Module Analysis

In this experiment, we conducted a comprehensive analysis of NHL from multiple perspectives, including (i) The adaptation to transformer backbones, (ii) hyper-parameter analysis, (iii) gradient analysis, and (iv) More code length settings. We use CSQ as the deep hashing model in the following analysis.

5.7.1 Adaptation to Transformer Backbones. The proposed NHL module can be integrated into the majority of deep supervised hashing models. In most deep hashing models, deep convolutional neural networks like ResNet50 [14] are used to extract the image

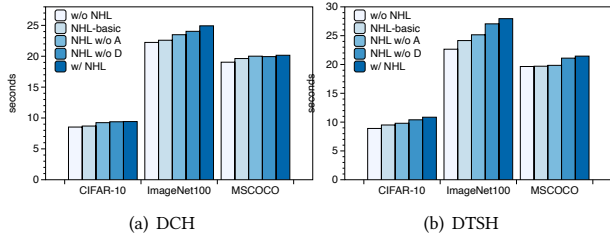


Figure 4: The average training time per epoch for CSQ and DCH on three datasets, when they use the original hash layer, NHL, or the variants of NHL.

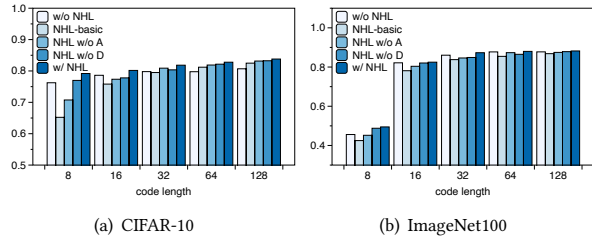


Figure 5: The $mAP@K$ results with NHL variants on CIFAR-10 and ImageNet100 datasets.

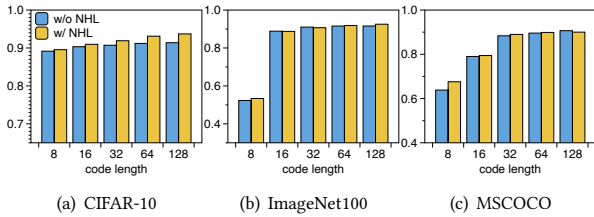


Figure 6: The $mAP@K$ evaluation when using ViT as the backbone of CSQ in three datasets. The blue bar denotes CSQ w/o NHL, while yellow denotes CSQ w/ NHL.

feature, and ResNet50 also served as the backbone for our prior experiments. Recently, the transformer architecture has achieved success in various fields. Some studies [11, 17] on deep hashing have explored the ViT [8] to extract the image feature and get better results. To evaluate the compatibility of the NHL with the transformer backbone, we used ViT_B_16 as the backbone of the CSQ model. Figure 6 shows the results, revealing that the NHL remains effective when integrated with the ViT_B_16 backbone, signifying that our proposed NHL is equally applicable to the current transformer architectures.

5.7.2 Parameter Sensitivity. In Eq.(11), λ serves as a hyper-parameter that governs the balance of the long-short cascade self-distillation. We evaluated its values from $\{10^1, 10^0, 10^{-1}, 10^{-2}, 10^{-3}\}$ to calculate the $mAP@K$ across three datasets when using CSQ as the deep hashing model. Figure 7 depicts the results and reveals that

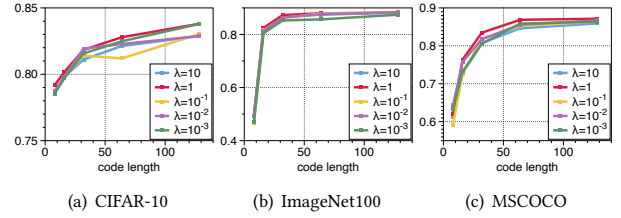


Figure 7: The $mAP@K$ results when using various λ in three datasets. It shows that NHL is not sensitive to λ .

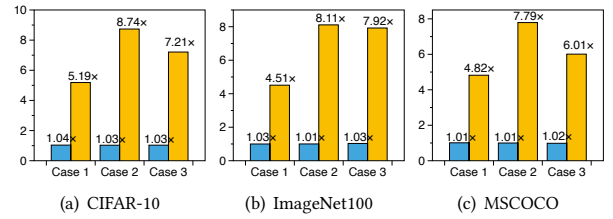


Figure 8: The analysis on more code length settings. The blue bars denote the average ratio of $mAP@K$ at various lengths with and without using NHL. The yellow bars denote the time cost ratio to complete training with and without using NHL.

NHL’s performance exhibits remarkable robustness to variations in λ . Thus, this finding suggests that the NHL can be seamlessly integrated into many scenarios with minimal adjustment.

5.7.3 More Code Length Settings. In prior experiments, we configured the hash codes to the five most commonly used lengths within the deep hashing model. This experiment explores the results under a broader range of code length settings. To this end, we established three scenarios for code length:

- **Case 1** set a code length at every 32-bit interval, that is, $b = \{32 \times k\}_{k=1}^4$ and $m = 4$.
- **Case 2** set a code length at every 16-bit interval, that is, $b = \{16 \times k\}_{k=1}^8$ and $m = 8$.
- **Case 3** set a code length at every 8-bit interval, that is, $b = \{8 \times k\}_{k=1}^{16}$ and $m = 16$.

We use CSQ as the deep hashing model. Figure 8 presents the corresponding results. Here, the blue bars represent the average ratio of $mAP@K$ at various lengths with and without using NHL. The yellow bars indicate the time cost ratio to complete training with and without using NHL. We observe that even with different code length settings, the use of NHL ensures a reduction in overall training time and improves the code quality. Moreover, it is noteworthy that the total training time does not monotonically increase with the number of output code lengths. For instance, the efficiency enhancement ratio in Setting 3 is not as high as in Setting 2. This is attributed to the requirement for the model to undergo more training iterations in Setting 3 to ensure favorable outcomes across a greater number of code lengths.

6 Conclusion

In this paper, we proposed a plug-and-play module NHL for deep hashing models. NHL enables deep hashing models to simultaneously generate hash codes of various lengths, thereby streamlining the training process and reducing the computational burden. Besides, the introduced adaptive weights strategy and the long-short cascade self-distillation ensure the effectiveness of NHL. We conducted extensive experiments on three datasets to evaluate the performance of the NHL. The results demonstrate that NHL accelerates the training process and maintains or enhances retrieval effectiveness across various deep supervised hashing models. In addition to its application in large-scale image retrieval, hashing has also found widespread use in other domains, including cross-modal retrieval [32, 41, 48], multi-modal retrieval [53, 57], and other essential applications [15, 33, 51]. Therefore, adapting Nested Hash Layer (NHL) to other domains is a research direction worth exploring.

References

- [1] Felix JS Bragman, Ryutarō Tanno, Sebastian Ourselin, Daniel C Alexander, and Jorge Cardoso. 2019. Stochastic filter groups for multi-task cnns: Learning specialist and generalist convolution kernels. In *Proceedings of the IEEE/CVF International Conference on Computer Vision*. 1385–1394.
- [2] Fatih Cakir, Kun He, Sarah Adel Bargal, and Stan Sclaroff. 2019. Hashing with mutual information. *IEEE transactions on pattern analysis and machine intelligence* 41, 10 (2019), 2424–2437.
- [3] Yue Cao, Mingsheng Long, Bin Liu, and Jianmin Wang. 2018. Deep cauchy hashing for hamming space retrieval. In *Proceedings of the IEEE Conference on Computer Vision and Pattern Recognition*. 1229–1237.
- [4] Yudong Chen, Zhihui Lai, Yujuan Ding, Kaiyi Lin, and Wai Keung Wong. 2019. Deep supervised hashing with anchor graph. In *Proceedings of the IEEE/CVF international conference on computer vision*. 9796–9804.
- [5] Zhao Chen, Vijay Badrinarayanan, Chen-Yu Lee, and Andrew Rabinovich. 2018. Gradnorm: Gradient normalization for adaptive loss balancing in deep multitask networks. In *International conference on machine learning*. PMLR, 794–803.
- [6] Zhao Chen, Jiquan Ngiam, Yanping Huang, Thang Luong, Henrik Kretzschmar, Yuning Chai, and Dragomir Anguelov. 2020. Just pick a sign: Optimizing deep multitask models with gradient sign dropout. *Advances in Neural Information Processing Systems* 33 (2020), 2039–2050.
- [7] Jia Deng, Wei Dong, Richard Socher, Li-Jia Li, Kai Li, and Li Fei-Fei. 2009. Imagenet: A large-scale hierarchical image database. In *2009 IEEE conference on computer vision and pattern recognition*. Ieee, 248–255.
- [8] Alexey Dosovitskiy, Lucas Beyer, Alexander Kolesnikov, Dirk Weissenborn, Xi-aohua Zhai, Thomas Unterthiner, Mostafa Dehghani, Matthias Minderer, Georg Heigold, Sylvain Gelly, et al. 2020. An Image is Worth 16x16 Words: Transformers for Image Recognition at Scale. In *International Conference on Learning Representations*.
- [9] Lixin Fan, Kam Woh Ng, Ce Ju, Tianyu Zhang, and Chee Seng Chan. 2020. Deep Polarized Network for Supervised Learning of Accurate Binary Hashing Codes.. In *IJCAI*. 825–831.
- [10] Yuan Gao, Haoping Bai, Zequn Jie, Jiayi Ma, Kui Jia, and Wei Liu. 2020. Mtl-nas: Task-agnostic neural architecture search towards general-purpose multi-task learning. In *Proceedings of the IEEE/CVF Conference on computer vision and pattern recognition*. 11543–11552.
- [11] Qinkang Gong, Liangdao Wang, Hanjiang Lai, Yan Pan, and Jian Yin. 2022. Vit2hash: unsupervised information-preserving hashing. *arXiv preprint arXiv:2201.05541* (2022).
- [12] SHI Guangyuan, Qimai Li, Wenlong Zhang, Jiabin Chen, and Xiao-Ming Wu. 2022. Recon: Reducing Conflicting Gradients From the Root For Multi-Task Learning. In *The Eleventh International Conference on Learning Representations*.
- [13] Michelle Guo, Albert Haque, De-An Huang, Serena Yeung, and Li Fei-Fei. 2018. Dynamic task prioritization for multitask learning. In *Proceedings of the European conference on computer vision (ECCV)*. 270–287.
- [14] Kaiming He, Xiangyu Zhang, Shaoqing Ren, and Jian Sun. 2016. Deep residual learning for image recognition. In *Proceedings of the IEEE conference on computer vision and pattern recognition*. 770–778.
- [15] Liyang He, Zhenya Huang, Enhong Chen, Qi Liu, Shiwei Tong, Hao Wang, Defu Lian, and Shijin Wang. 2023. An efficient and robust semantic hashing framework for similar text search. *ACM Transactions on Information Systems* 41, 4 (2023), 1–31.
- [16] Liyang He, Zhenya Huang, Chenglong Liu, Rui Li, Runze Wu, Qi Liu, and Enhong Chen. 2024. One-bit Deep Hashing: Towards Resource-Efficient Hashing Model with Binary Neural Network. In *Proceedings of the 32nd ACM International Conference on Multimedia*. 7162–7171.
- [17] Liyang He, Zhenya Huang, Jiayu Liu, Enhong Chen, Fei Wang, Jing Sha, and Shijin Wang. 2024. Bit-mask Robust Contrastive Knowledge Distillation for Unsupervised Semantic Hashing. *arXiv preprint arXiv:2403.06071* (2024).
- [18] Jiun Tian Hoe, Kam Woh Ng, Tianyu Zhang, Chee Seng Chan, Yi-Zhe Song, and Tao Xiang. 2021. One loss for all: Deep hashing with a single cosine similarity based learning objective. *Advances in Neural Information Processing Systems* 34 (2021), 24286–24298.
- [19] Qing-Yuan Jiang and Wu-Jun Li. 2018. Asymmetric deep supervised hashing. In *Proceedings of the AAAI conference on artificial intelligence*, Vol. 32.
- [20] Alex Kendall, Yarin Gal, and Roberto Cipolla. 2018. Multi-task learning using uncertainty to weigh losses for scene geometry and semantics. In *Proceedings of the IEEE conference on computer vision and pattern recognition*. 7482–7491.
- [21] Diederik P Kingma and Jimmy Ba. 2014. Adam: A method for stochastic optimization. *arXiv preprint arXiv:1412.6980* (2014).
- [22] Iasonas Kokkinos. 2017. Ubernet: Training a universal convolutional neural network for low-, mid-, and high-level vision using diverse datasets and limited memory. In *Proceedings of the IEEE conference on computer vision and pattern recognition*. 6129–6138.
- [23] Alex Krizhevsky, Geoffrey Hinton, et al. 2009. Learning multiple layers of features from tiny images. (2009).
- [24] Aditya Kusupati, Gantavya Bhatt, Aniket Rege, Matthew Wallingford, Aditya Sinha, Vivek Ramanujan, William Howard-Snyder, Kaifeng Chen, Sham Kakade, Prateek Jain, et al. 2022. Matryoshka representation learning. *Advances in Neural Information Processing Systems* 35 (2022), 30233–30249.
- [25] Taeho Lee and Junhee Seok. 2023. Multi Task Learning: A Survey and Future Directions. In *2023 International Conference on Artificial Intelligence in Information and Communication (ICAIC)*. IEEE, 232–235.
- [26] Y Li, W Pei, Yufei Zha, and JC van Gemert. 2020. Push for quantization: Deep fisher hashing. In *30th British Machine Vision Conference, BMVC 2019*.
- [27] Tsung-Yi Lin, Michael Maire, Serge Belongie, James Hays, Pietro Perona, Deva Ramanan, Piotr Dollár, and C Lawrence Zitnick. 2014. Microsoft coco: Common objects in context. In *Computer Vision—ECCV 2014: 13th European Conference, Zurich, Switzerland, September 6–12, 2014, Proceedings, Part V 13*. Springer, 740–755.
- [28] Bin Liu, Yue Cao, Mingsheng Long, Jianmin Wang, and Jingdong Wang. 2018. Deep triplet quantization. In *Proceedings of the 26th ACM international conference on Multimedia*. 755–763.
- [29] Bo Liu, Xingchao Liu, Xiaojie Jin, Peter Stone, and Qiang Liu. 2021. Conflict-averse gradient descent for multi-task learning. *Advances in Neural Information Processing Systems* 34 (2021), 18878–18890.
- [30] Haomiao Liu, Ruiping Wang, Shiguang Shan, and Xilin Chen. 2016. Deep supervised hashing for fast image retrieval. In *Proceedings of the IEEE conference on computer vision and pattern recognition*. 2064–2072.
- [31] Shikun Liu, Edward Johns, and Andrew J Davison. 2019. End-to-end multi-task learning with attention. In *Proceedings of the IEEE/CVF conference on computer vision and pattern recognition*. 1871–1880.
- [32] Yishu Liu, Qingpeng Wu, Zheng Zhang, Jingyi Zhang, and Guangming Lu. 2023. Multi-Granularity Interactive Transformer Hashing for Cross-modal Retrieval. In *Proceedings of the 31st ACM International Conference on Multimedia*. 893–902.
- [33] Xin Lu, Shikun Chen, Yichao Cao, Xin Zhou, and Xiaobo Lu. 2023. Attributes Grouping and Mining Hashing for Fine-Grained Image Retrieval. In *Proceedings of the 31st ACM International Conference on Multimedia*. 6558–6566.
- [34] Xiao Luo, Haixin Wang, Daqing Wu, Chong Chen, Minghua Deng, Jianqiang Huang, and Xian-Sheng Hua. 2023. A survey on deep hashing methods. *ACM Transactions on Knowledge Discovery from Data* 17, 1 (2023), 1–50.
- [35] Yadan Luo, Zi Huang, Yang Li, Fumin Shen, Yang Yang, and Peng Cui. 2020. Collaborative learning for extremely low bit asymmetric hashing. *IEEE Transactions on Knowledge and Data Engineering* 33, 12 (2020), 3675–3685.
- [36] Devraj Mandal, Yashas Annadani, and Soma Biswas. 2019. Growbit: Incremental hashing for cross-modal retrieval. In *Computer Vision—ACCV 2018: 14th Asian Conference on Computer Vision, Perth, Australia, December 2–6, 2018, Revised Selected Papers, Part IV 14*. Springer, 305–321.
- [37] Zexuan Qiu, Qinliang Su, Zijing Ou, Jianxing Yu, and Changyou Chen. 2021. Unsupervised hashing with contrastive information bottlenecking. In *Proceedings of the Thirtieth International Joint Conference on Artificial Intelligence, IJCAI 2021, Virtual Event / Montreal, Canada, 19–27 August 2021*. 959–965.
- [38] Sebastian Ruder, Joachim Bingel, Isabelle Augenstein, and Anders Søgaard. 2019. Latent multi-task architecture learning. In *Proceedings of the AAAI conference on artificial intelligence*, Vol. 33. 4822–4829.
- [39] Fumin Shen, Xin Gao, Li Liu, Yang Yang, and Heng Tao Shen. 2017. Deep asymmetric pairwise hashing. In *Proceedings of the 25th ACM international conference on Multimedia*. 1522–1530.
- [40] Yuan Sun, Dezhong Peng, Jian Dai, and Zhenwen Ren. 2023. Stepwise Refinement Short Hashing for Image Retrieval. In *Proceedings of the 31st ACM International Conference on Multimedia*. 6501–6509.

- [41] Rong-Cheng Tu, Xian-Ling Mao, Bing Ma, Yong Hu, Tan Yan, Wei Wei, and Heyan Huang. 2020. Deep cross-modal hashing with hashing functions and unified hash codes jointly learning. *IEEE Transactions on Knowledge and Data Engineering* 34, 2 (2020), 560–572.
- [42] Liangdao Wang, Yan Pan, Hanjiang Lai, and Jian Yin. 2022. Image Retrieval with Well-Separated Semantic Hash Centers. In *Proceedings of the Asian Conference on Computer Vision*. 978–994.
- [43] Liangdao Wang, Yan Pan, Cong Liu, Hanjiang Lai, Jian Yin, and Ye Liu. 2023. Deep Hashing With Minimal-Distance-Separated Hash Centers. In *Proceedings of the IEEE/CVF Conference on Computer Vision and Pattern Recognition*. 23455–23464.
- [44] Xiaofang Wang, Yi Shi, and Kris M Kitani. 2017. Deep supervised hashing with triplet labels. In *Computer Vision—ACCV 2016: 13th Asian Conference on Computer Vision, Taipei, Taiwan, November 20–24, 2016, Revised Selected Papers, Part I 13*. Springer, 70–84.
- [45] Dayan Wu, Qi Dai, Bo Li, and Weiping Wang. 2023. Deep uncoupled discrete hashing via similarity matrix decomposition. *ACM Transactions on Multimedia Computing, Communications and Applications* 19, 1 (2023), 1–22.
- [46] Dayan Wu, Qinghang Su, Bo Li, and Weiping Wang. 2022. Efficient hash code expansion by recycling old bits. In *Proceedings of the 30th ACM International Conference on Multimedia*. 572–580.
- [47] Dayan Wu, Qinghang Su, Bo Li, and Weiping Wang. 2024. Pairwise-Label-Based Deep Incremental Hashing with Simultaneous Code Expansion. In *Proceedings of the AAAI Conference on Artificial Intelligence*, Vol. 38. 9169–9177.
- [48] De Xie, Cheng Deng, Chao Li, Xianglong Liu, and Dacheng Tao. 2020. Multi-task consistency-preserving adversarial hashing for cross-modal retrieval. *IEEE Transactions on Image Processing* 29 (2020), 3626–3637.
- [49] Tianhe Yu, Saurabh Kumar, Abhishek Gupta, Sergey Levine, Karol Hausman, and Chelsea Finn. 2020. Gradient surgery for multi-task learning. *Advances in Neural Information Processing Systems* 33 (2020), 5824–5836.
- [50] Li Yuan, Tao Wang, Xiaopeng Zhang, Francis EH Tay, Zequn Jie, Wei Liu, and Jiashi Feng. 2020. Central similarity quantization for efficient image and video retrieval. In *Proceedings of the IEEE/CVF conference on computer vision and pattern recognition*. 3083–3092.
- [51] Chong-Yu Zhang, Xin Luo, Yu-Wei Zhan, Peng-Fei Zhang, Zhen-Duo Chen, Yongxin Wang, Xun Yang, and Xin-Shun Xu. 2023. Self-Distillation Dual-Memory Online Hashing with Hash Centers for Streaming Data Retrieval. In *Proceedings of the 31st ACM International Conference on Multimedia*. 6340–6349.
- [52] Shu Zhao, Dayan Wu, Wanqian Zhang, Yu Zhou, Bo Li, and Weiping Wang. 2020. Asymmetric deep hashing for efficient hash code compression. In *Proceedings of the 28th ACM International Conference on Multimedia*. 763–771.
- [53] Chaoqun Zheng, Lei Zhu, Xu Lu, Jingjing Li, Zhiyong Cheng, and Hanwang Zhang. 2019. Fast discrete collaborative multi-modal hashing for large-scale multimedia retrieval. *IEEE Transactions on Knowledge and Data Engineering* 32, 11 (2019), 2171–2184.
- [54] Xiangtao Zheng, Yichao Zhang, and Xiaoqiang Lu. 2020. Deep balanced discrete hashing for image retrieval. *Neurocomputing* 403 (2020), 224–236.
- [55] Hao Zhu, Shenghua Gao, et al. 2017. Locality Constrained Deep Supervised Hashing for Image Retrieval. In *IJCAI*. 3567–3573.
- [56] Han Zhu, Mingsheng Long, Jianmin Wang, and Yue Cao. 2016. Deep hashing network for efficient similarity retrieval. In *Proceedings of the AAAI conference on Artificial Intelligence*, Vol. 30.
- [57] Lei Zhu, Xu Lu, Zhiyong Cheng, Jingjing Li, and Huaxiang Zhang. 2020. Deep collaborative multi-view hashing for large-scale image search. *IEEE Transactions on Image Processing* 29 (2020), 4643–4655.